Chemical Science

ROYAL SOCIETY OF CHEMISTRY

EDGE ARTICLE

View Article Online
View Journal | View Issue

Check for updates

Cite this: *Chem. Sci.*, 2020, **11**, 9115

All publication charges for this article have been paid for by the Royal Society of Chemistry

Received 10th June 2020
Accepted 22nd July 2020

DOI: 10.1039/d0sc03227a

rsc.li/chemical-science

Catalytic enantioselective allene–anhydride approach to β,γ-unsaturated enones bearing an α-all-carbon-quarternary center†

Yuan Yuan,[a] Xue Zhang,[*b] Hui Qian[*a] and Shengming Ma[*ab]

A protocol of highly regio- and enantioselective copper-catalyzed hydroacylation of the non-terminal C=C bond in 1,1-disubstituted terminal allenes with anhydrides has been developed. Both aromatic and aliphatic carboxylic anhydrides are applicable to the efficient construction of all carbon quarternary centers connected with a versatile C=C bond and a useful ketone functionality. The synthetic potentials of the enantioenriched products have also been demonstrated. Density functional theory (DFT) calculations were performed to explain the steric outcome of the products: the hydroacylation proceeds through a six-membered transition state and the ligand-substrate steric interactions account for the observed enantioselectivity although the chiral ligand is far away from the to-be-genetated chiral center.

Open Access Article. Published on 22 July 2020. Downloaded on 2/7/2026 4:41:18 PM.
This article is licensed under a Creative Commons Attribution-NonCommercial 3.0 Unported Licence.

Introduction

Carboxylic anhydrides are readily available, stable, easy-to-handle, and widely used as the acyl source to afford ketones by treatment with organomagnesium, lithium, or zinc reagents (Scheme 1A-a).[1] However, the challenge lies in the formation of tertiary alcohols as by-products *via* over-addition to the *in situ* formed ketones.[2] Miura,[3a] Krische,[3b] (Scheme 1A-b), Buchwald (Scheme 1A-c)[4] and their coworkers reported such transition metal-catalyzed reactions of aryl anhydrides with *in situ* generated organometallic reagents from hydrometalation of styrenes with different hydride donors offering exclusive approaches from carboxylic anhydrides to ketones. On the other hand, attention has been paid to the corresponding reactions involving allenes[5,6] with anhydrides: in 2015, Fujihara and Tsuji reported the Pd-catalyzed formal hydroacylation of mono-substituted terminal allenes with aryl carboxylic anhydrides to afford α,β-unsaturated enones (Scheme 1A-d).[7] In 2018, Tsuji and coworkers reported a copper-catalyzed boroacylation of 1,1-disubstituted allenes[8] with carboxylic anhydrides, which provide an access to racemic β-boryl-β,γ-unsaturated ketones bearing an all-carbon quarternary center in good to high yields (Scheme 1A-e).[9–11] We herein wish to present the first example of highly regio- and enantioselective hydrocupration of 1,1-disubstituted allenes followed by trapping with both aryl and alkyl carboxylic anhydrides to afford optically active β,γ-unsaturated enones bearing an α-all-carbon-quarternary stereocenter, which are challenging to construct (Scheme 1B).[12–16] It should be mentioned that the formation of regioisomeric α,β-unsaturated ketones was not observed.

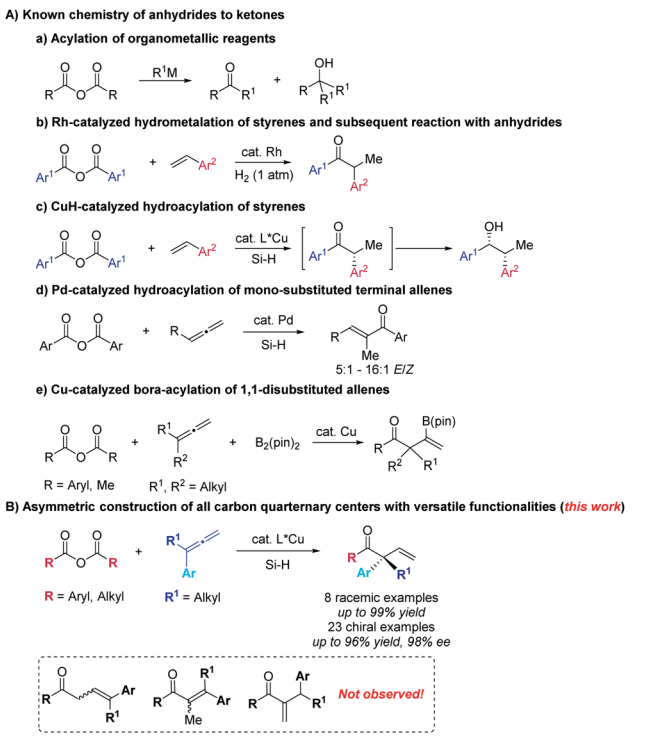

Scheme 1 Acylations with carboxylic anhydrides as acyl source.

[a]*Research Center for Molecular Recognition and Synthesis, Department of Chemistry, Fudan University, 220 Handan Lu, Shanghai 200433, P. R. China. E-mail: qian_hui@fudan.edu.cn*

[b]*State Key Laboratory of Organometallic Chemistry, Shanghai Institute of Organic Chemistry, Chinese Academy of Sciences, 345 Lingling Lu, Shanghai 200032, P. R. China. E-mail: masm@sioc.ac.cn*

† Electronic supplementary information (ESI) available. CCDC 1939837. For ESI and crystallographic data in CIF or other electronic format see DOI: 10.1039/d0sc03227a

Open Access Article. Published on 22 July 2020. Downloaded on 2/7/2026 4:41:18 PM.
This article is licensed under a Creative Commons Attribution-NonCommercial 3.0 Unported Licence.

Results and discussion

Initially, we studied the reaction of $Cu(OAc)_2$-catalyzed hydroacylation of 1,1-disubstituted allene **1a**[17] with carboxylic acid anhydride **2a** *via* brief screening of non-chiral ligands and solvents (Table 1). Commercially available bidentate ligands such as DPPM, DPPE, DPPP, DPPF, and BINAP were examined and we were delighted to find DPPE could afford 31% yield of the desired β,γ-unsaturated enone *rac*-**3aa** (entries 1–5). PCy_3 led to full recovery of starting material **1a** (entry 6). Studies on the effect of solvents with DPPE as the ligand indicated that the reactions in dioxane, dichloromethane, and toluene afforded the expected product *rac*-**3aa** in low yields (entries 8–10) and the best solvent is THF. After further optimization, it was observed that the reaction utilizing 0.5 mmol anhydride **2a**, 2.0 equiv. of allene **1a**, 2.5 mol% of $Cu(OAc)_2$, 2.5 mol% of DPPE, and 3.0 equiv. of $Me(MeO)_2SiH$ in THF at room temperature for 6.0 h could afford *rac*-**3aa** in 66% yield (entry 12).

The scope of this reaction was then demonstrated and the typical results were shown in Table 2. Racemic β,γ-unsaturated enones *rac*-**3** were obtained in good to excellent yields and the reaction is amenable to both terminal 1-electron-withdrawing or electron-donating group substituted aryl-1-alkylallenes and differently substituted aryl anhydrides (*m*-Me, *p*-F, *p*-Cl, and *p*-*t*-Bu).

Table 1 Optimization for the Cu-catalyzed reaction of **1a** with anhydride **2a**[a]

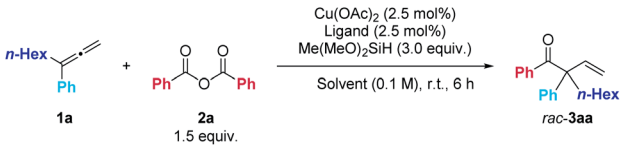

Entry	Ligand	Solvent	NMR yield of *rac*-**3aa** (%)	Recovery of **1a** (%)
1	DPPM	THF	0	100
2	DPPE	THF	31	63
3	DPPP	THF	0	100
4	DPPF	THF	8	84
5	BINAP	THF	21	75
6[b]	PCy_3	THF	0	100
7	DPPE	Cyclohexane	0	100
8	DPPE	Dioxane	15	78
9	DPPE	DCM	10	79
10	DPPE	Toluene	24	62
11[c]	DPPE	THF	49	4
12[d]	DPPE	THF	66	—

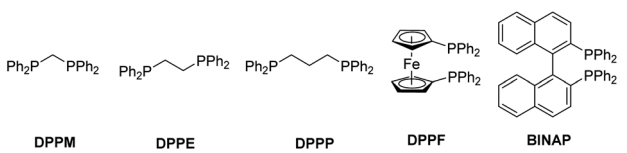

[a] Reaction conditions: allene **1a** (0.1 mmol), anhydride **2a** (1.5 equiv.), $Cu(OAc)_2$ (2.5 mol%), ligand (2.5 mol%), and $Me(MeO)_2SiH$ (3.0 equiv.) in solvent (1.0 mL) at room temperature for 6 h. [b] PCy_3 (5.0 mol%) was used. [c] Allene **1a** (0.5 mmol) and **2a** (1.5 equiv.) were used. [d] Allene **1a** (2.0 equiv.) and **2a** (0.5 mmol) were used.

Table 2 Substrate scope for the racemic version of Cu-catalyzed reaction of allenes with anhydrides[a]

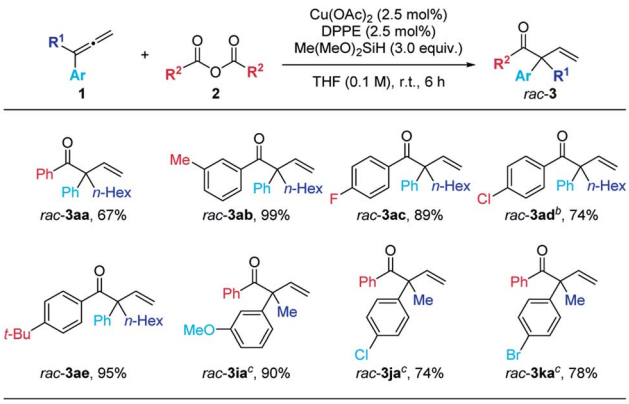

[a] Reaction conditions: allene **1** (2.0 equiv.), anhydride **2** (0.5 mmol), $Cu(OAc)_2$ (2.5 mol%), DPPE (2.5 mol%), and $Me(MeO)_2SiH$ (3.0 equiv.) in THF (10.0 mL) at room temperature for 6 h. [b] The reaction was carried out for 9 h. [c] Allene **1** (1.5 equiv.) and **2** (0.5 mmol) were used.

Encouraged by these results, we turned our efforts to develop the enantioselective reaction by using 3-phenyl-nona-1,2-diene (**1a**) and benzoic anhydride (**2a**) as the model substrates again (Table 3). To our delight, when (*R*)-BINAP was used as the chiral ligand, the desired product **3aa** was obtained in 74% NMR yield with 79% ee. Biaryl-based (*R*)-MeO-Biphep, (*R*)-C3-Tunephos,

Table 3 Ligand screening[a]

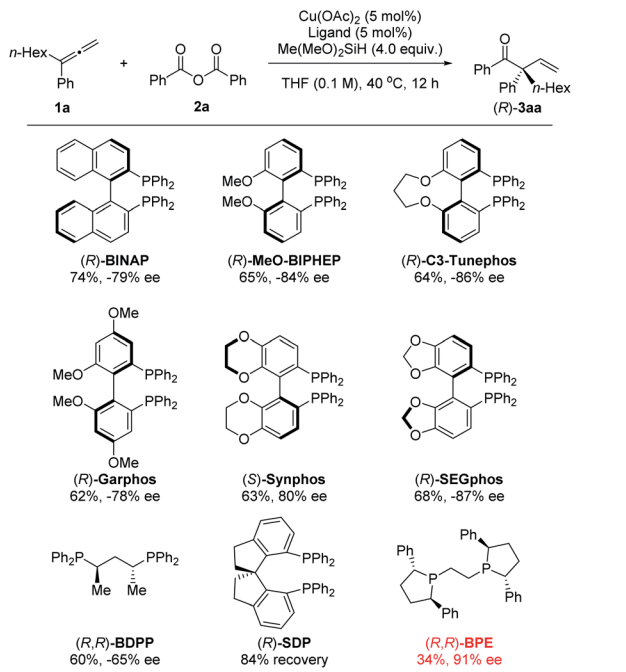

[a] Reaction conditions: **1a** (0.1 mmol), **2a** (1.5 equiv.), $Cu(OAc)_2$ (5 mol%), ligand (5 mol%), and $Me(MeO)_2SiH$ (4.0 equiv.) in THF (1.0 mL) at 40 °C for 12 h. Yield was determined by ^1H NMR analysis using dibromomethane as the internal standard.

This journal is © The Royal Society of Chemistry 2020

Open Access Article. Published on 22 July 2020. Downloaded on 2/7/2026 4:41:18 PM.
This article is licensed under a Creative Commons Attribution-NonCommercial 3.0 Unported Licence.

(*R*)-Garphos, (*S*)-Synphos, and (*R*)-Segphos could afford the desired product **3aa** in good yield with 78–87% ee. Non-rigid (*R*,*R*)-BDPP could also give a moderate enantio-selectivity while the spiro-ligand (*R*)-SDP was not working for this reaction. Finally, we had identified successfully (*R*,*R*)-BPE as a promising ligand, affording (*R*)-**3aa** in 34% NMR yield with 91% ee.

When the reaction was conducted at room temperature, both the yield and ee value increased (Table 4, entry 1). Shortening the reaction time to 5 h improved the yield to 92% with 96% ee (Table 4, entry 2). Three equivalents of $Me(MeO)_2SiH$ were still efficient for this process (Table 4, entry 3). However, recovery of **1a** was observed when further decreasing the loading of silane (Table 4, entries 4 & 5). When the reaction was conducted on 1.0 mmol scale for 6 h, the loading of $Cu(OAc)_2$ and (*R*,*R*)-BPE could be reduced to 2.5 mol% affording (*R*)-**3aa** in 86% NMR yield with 95% ee, which was chosen as the optimal reaction conditions (Table 4, entry 6).

With the optimized conditions in hand, we next examined the scope of this enantioselective reaction. As shown in Table 5, a wide range of terminal 1,1-disubstituted allenes bearing one aryl group and one alkyl group reacted smoothly with **2a** to form the corresponding β,γ-unsaturated enone products (*R*)-**3** with excellent enantioselectivity. The absolute configuration of these products has been established *via* X-ray crystallography of (*R*)-**3ea**. Allenes with the aryl group (Ar) bearing different substituents, including alkoxy group and halides, are all suitable substrates ((*R*)-**3fa** to (*R*)-**3ka**). Furthermore, the substrate scope of carboxylic anhydrides with allene **1a** was examed. Both electron-rich and electron-deficient aryl carboxylic anhydrides gave the products in high to excellent yields and ees ((*R*)-**3ab** to (*R*)-**3ag**). It is worth mentioning that alkyl carboxylic acid anhydrides also worked well under the optimized conditions to afford the desired products with excellent enantioselectivity ((*R*)-**3ah–3aj**). When (*S*,*S*)-BPE was used as the ligand, the enantiomers could be obtained ((*S*)-**3af**, (*S*)-**3ai**, and (*S*)-**3aj**). In all these reactions, only the more substituted C=C bond in allene reacted formally.

The practicality of this reaction has been demonstrated by executing a 10.0 mmol scale reaction, affording 2.4974 g of (*R*)-**3ka** in 79% yield with 96% ee (Scheme 2a). The highly functionalized products could be easily transformed to other useful molecules (Scheme 2b): after treatment with hydroxylamine hydrochloride,[18] the β,γ-unsaturated enone could be transformed to β,γ-unsaturated ketoxime (*R*,*Z*)-**4**, which was reported to be very useful and convenient starting material for the synthesis of isoxazoline.[18,19] The aryl–Br bond could undergo Suzuki coupling to afford (*R*)-**5** in 90% yield with 96% ee. The carbon–carbon double bond may undergo aldehyde-selective Wacker-type oxidation and hydrogenation to form the corresponding products (*R*)-**6** [20] and (*R*)-**7** in excellent enantiomeric excess.

Table 4 Further optimization of the reaction conditions[a]

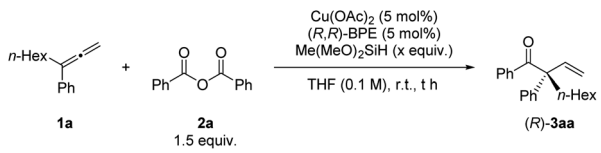

Entry	*x*	*t* (h)	Recovery of **1a**[b] (%)	NMR yield of **3aa**[b] (%)	ee (%)
1	4.0	12	—	68	93
2	4.0	5	—	92	96
3	3.0	5	—	89	94
4	2.0	5	15	82	94
5	1.0	5	50	50	94
6[c,d]	3.0	6	—	86	95

[a] Reaction conditions: **1a** (0.1 mmol), **2a** (0.15 mmol), $Cu(OAc)_2$ (5 mol%), (*R*,*R*)-BPE (5 mol%), and $Me(MeO)_2SiH$ in THF (1.0 mL) at room temperature unless otherwise noted. [b] Determined by ^1H NMR analysis using $MeNO_2$ as the internal standard. [c] The reaction was conducted using $Cu(OAc)_2$ (2.5 mol%) and (*R*,*R*)-BPE (2.5 mol%). [d] The reaction was conducted on 1.0 mmol scale.

Table 5 Scope of allenes and anhydrides[a]

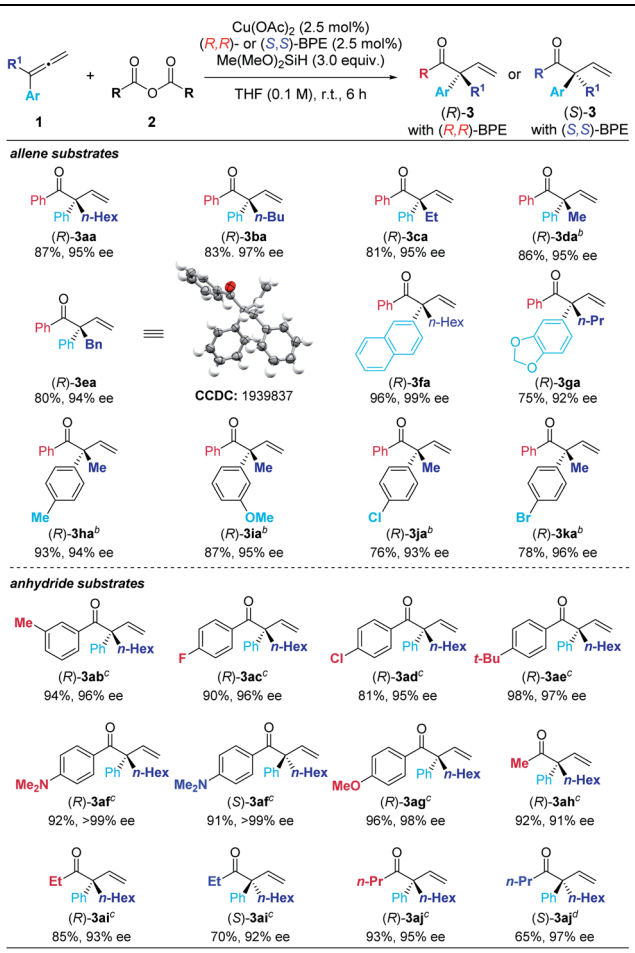

[a] Reaction conditions: allene **1** (1.0 mmol), anhydride **2** (1.5 equiv.), $Cu(OAc)_2$ (2.5 mol%), (*R*,*R*)-BPE (2.5 mol%) and $Me(MeO)_2SiH$ (3.0 equiv.) in THF (10.0 mL) at room temperature for 6 h unless otherwise noted. [b] Allene **1** (1.5 equiv.), anhydride **2a** (1.0 mmol) and $Me(MeO)_2SiH$ (1.5 equiv.) were used instead. [c] Allene **1a** (2.0 equiv.), anhydride **2** (1.0 mmol) were used instead. [d] Allene **1a** (1.5 equiv.), anhydride **2** (0.5 mmol), and (*S*,*S*)-BPE (2.5 mol%) were used instead.

Open Access Article. Published on 22 July 2020. Downloaded on 2/7/2026 4:41:18 PM.
This article is licensed under a Creative Commons Attribution-NonCommercial 3.0 Unported Licence.

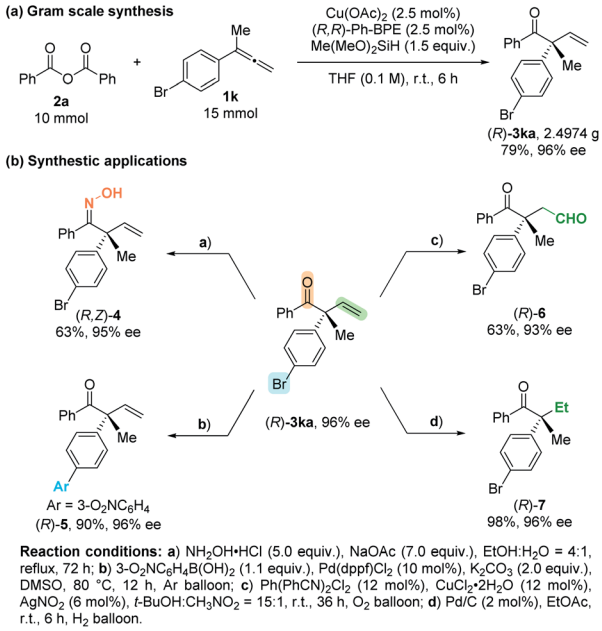

Scheme 2 Gram scale synthesis of (*R*)-**3ka** and its synthetic potentials.

A plausible catalytic cycle was proposed (Scheme 3): hydrocupration of the terminal C=C bond in allene **1d** with the *in situ* formed copper-hydride species **I** would generate the allyl copper specie *E*-**II**. Subsequent nucleophilic addition of *E*-**II** with anhydride **2a** would afford the copper species **III** *via* the six-membered ring chair-like transition state (**TS**). The β-O elimination of **III** would eventually regenerate the C=O bond affording enantioenriched (*R*)-**3da** and the Cu-OBz specie **IV**, which would react with $Me(MeO)_2SiH$ to regenerate copper-hydride **I** to finish the catalytic cycle.

It should be noted that the chiral ligand is far away from the to-be-generated chiral center as shown in the six-membered ring chair-like transition state (**TS**). To pursue a further understanding of the observed enantioselectivity of the current reaction, DFT calculations were performed at the M06/6-311+G(d,p)-SDD/SMD(THF)//B3LYP/6-31G(d)-LANL2DZ level, using allene **1d** and benzoic anhydride **2a** as the model substrates (see

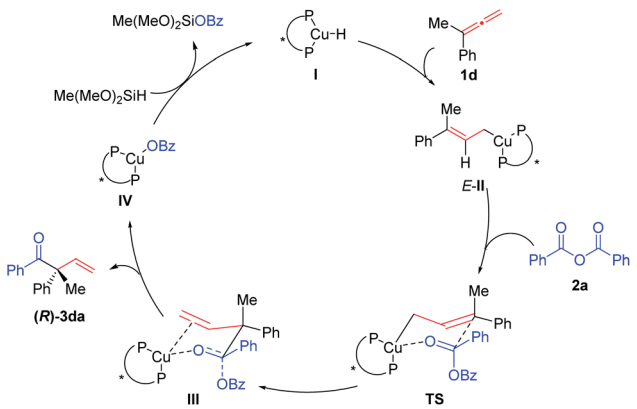

Scheme 3 The proposed mechanism.

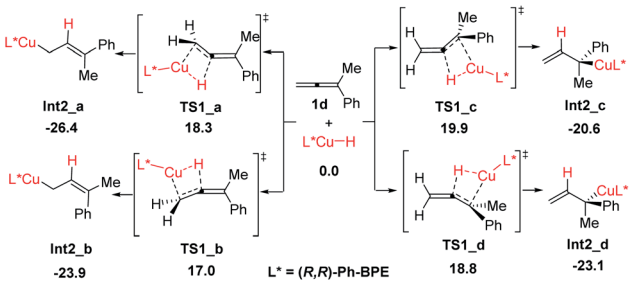

Scheme 4 Four competing transition structures associated with the hydro-cupration step. All energies are in kcal mol^{-1} with respect of CuH and allene (**1d**).

computational methods in the ESI for detailed information†). The reported energies are Gibbs energies that incorporate the effect of the THF solvent.

The reaction proceeds initially from the hydrocupration of allene **1d** with the *in situ* generated copper-hydride as shown in Scheme 4. Both terminal and internal double bonds of allene **1d** could participate in the hydrocupration, thus, four competing transition structures associated with the hydrocupration step are obtained, which are denoted as **TS1_a–d**, separately (see the ESI for other less favorable transition structures†). The activation barriers required for **TS1_a–d** are 18.3, 17.0, 19.9 and 18.8 kcal mol^{-1} respectively, indicating that this hydrocupration step favours terminal C=C bond over internal C=C bond in allene **1d**.

Four allylcoppers **Int2_a–d** could be provided irreversibly from the hydrocupration, among which the kinetically less favorable *E*-isomer of the terminal allylic copper **Int2_a** is the thermodynamically most stable. Further calculation reveals that **Int2_a–d** may isomerize to each other *via* 1,3-Cu shift (Scheme 5), and these interconversions are rather facial with barriers of less than 8 kcal mol^{-1}.

The subsequent addition of the benzoic anhydride to terminal allylic copper **Int2_a** or **Int2_b** could proceed *via* the six-membered cyclic chair-like transition states. The benzoic anhydride **2a** approaches from both faces of the prochiral center of **Int2_a** and **Int2_b**, leading to four six-membered transition states, which are denoted as **TS3_a1**, **TS3_a2**,

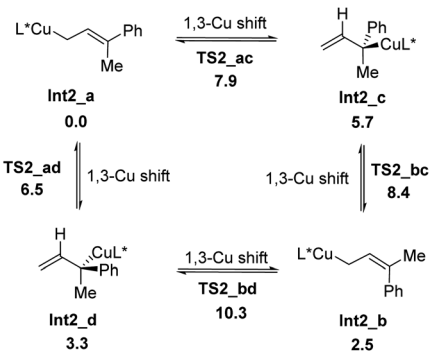

Scheme 5 The isomerization of **Int2_a–d**. All energies are in kcal mol^{-1} with respect of **Int2_a**.

This journal is © The Royal Society of Chemistry 2020

Open Access Article. Published on 22 July 2020. Downloaded on 2/7/2026 4:41:18 PM.
This article is licensed under a Creative Commons Attribution-NonCommercial 3.0 Unported Licence.

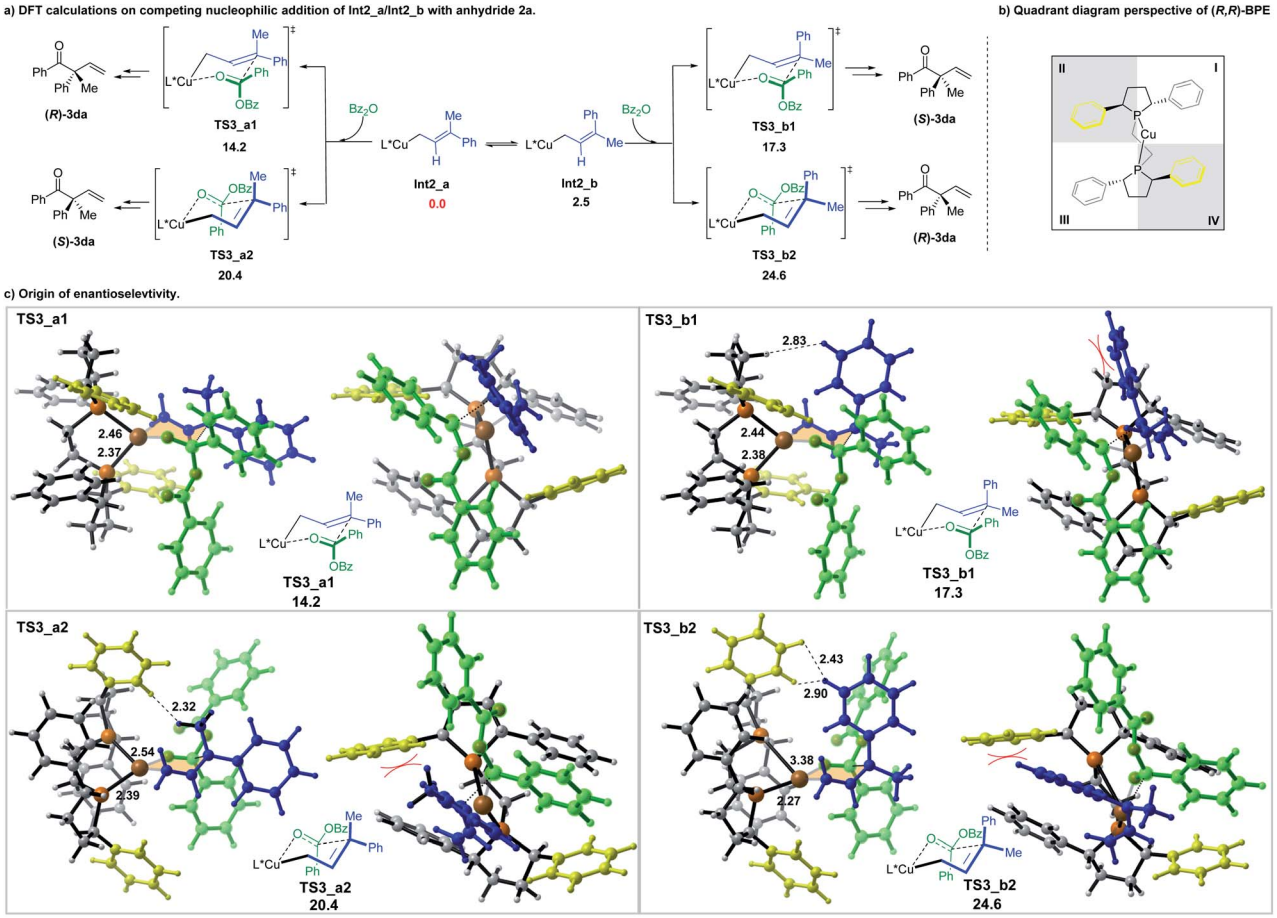

Scheme 6 The origin of enatioselectivity of the nucleophilic addition of **2a** to **Int2_a** and **Int2_b**. All energies are in kcal mol^{-1} with respect of **Int2_a**. Bond lengths are given in angstroms. The right side drawings in (c) are the views in quadrant as shown in (b).

TS3_b1 and **TS3_b2**, separately (Scheme 6a) (The benzoic anhydride **2a** participates with *Re*-face in these four transition states (see the ESI for the other four less favorable transition structures with *Si*-face **2a** participation†)). Geometry analysis of the six-membered transition structures indicates that **TS3** should be a late transition state (see the ESI for the detail†).

Among the four transition states, a *Re*-face approach of **2a** to the *E*-allyl intermediate **Int2_a** (**TS3_a1**, 14.2 kcal mol^{-1}), which leads to the formation of (*R*)-**3da**, is found to be the most favorable one, thus, accounting for the domination of the *R*-product observed in the experiment (Scheme 6).

The origin of the enantioselectivity can be visualized in the quadrant diagrams. Scheme 6b shows a quadrant diagram perspective of the (*R*,*R*)-BPE ligand, while Scheme 6c are the illustration of the four six-membered transition structures. In Scheme 6b, the phenyl groups in quadrants II and IV extend forward, which is in the same direction with the coordinated copper center, thus making these two locations more hindered than the other two. In the transition structures of **TS3_a1** and **TS3_a2**, which both originated from the *E*-allyl intermediate **Int2_a**, the smaller substituent (Me) locates at the pseudoaxial position of the chair-like six-member ring. The allyl moiety of **TS3_a1** is placed in the less hindered quadrant I. However, the methyl substituent of **TS3_a2** suffers an unfavourable steric repulsion with ligand phenyl group in quadrant II (H···H distance of only 2.32 Å), thus interpreting the preference of **TS3_a1** over **TS3_a2** by 6.2 kcal mol^{-1}. Alternatively, in **TS3_b1** and **TS3_b2**, associated with the *Z*-allyl intermediate **Int2_b**, the pseudoaxial occupation of the large phenyl group destabilizes both structures. The steric hindrance between the phenyl group and the carbon chain in phospha-five-membered-ring of ligand makes **TS3_b1** less favorable by 3.1 kcal mol^{-1} in energy than **TS3_a1**. Moreover, severe steric interaction between the pseudoaxial phenyl group and the ligand phenyl group in quadrant II further destabilizes **TS3_b2**, makes it the least stable one (10.4 kcal mol^{-1} higher in energy than **TS3_a1**). To reduce the steric repulsion, one phosphine is obliged to partly dissociate with the metal center, leading to the increasing of one of the Cu-P distance to 3.38 Å.

Conclusions

In summary, we have developed a highly efficient regio- and enantio-selective method for the construction of all carbon quarternary stereocenter linked with a C=C bond and a carbonyl group from 1,1-disubstituted allenes and carboxylic anhydrides. The current reaction represents the first copper-

Open Access Article. Published on 22 July 2020. Downloaded on 2/7/2026 4:41:18 PM. This article is licensed under a Creative Commons Attribution-NonCommercial 3.0 Unported Licence.

catalyzed enantioselective hydroacylation of allenes with carboxylic anhydrides. Enabled by the mild reaction conditions, the reactions proceed efficiently with good functional group compatibility. Synthetic transformations to other quarternary-carbon-center-containing molecules have also been established. Based on DFT calculations, the origin of the enantioselectivity has also been rationalized.

Conflicts of interest

There are no conflicts to declare.

Acknowledgements

Financial support from the National Natural Science Foundation of China (Grant No. 21690063 for S. Ma and Grant No. 21801041 for H. Qian) are greatly appreciated. We thank Mr Yizhan Zhai in this group for reproducing the results of *rac*-**3ae** presented in Table 2, and Mr Yulong Song in this group for reproducing the results of (*R*)-**3ea** and (*R*)-**3aj** in Table 5.

Notes and references

1 R. C. Larock, A. V. Dubrovskiy and N. A. Markina, in *Comprehensive Organic Transformations: A Guide to Functional Group Preparations*, 3rd edn, 2018, pp. 1–95.

2 Y. Miki, H. Hachiken and I. Yoshikawa, *Heterocycles*, 1997, **6**, 1143.

3 (*a*) K. Kokubo, M. Miura and M. Nomura, *Organometallics*, 1995, **14**, 4521; (*b*) Y.-T. Hong, A. Barchuk and M. J. Krische, *Angew. Chem., Int. Ed.*, 2006, **45**, 6885.

4 J. S. Bandar, E. Ascic and S. L. Buchwald, *J. Am. Chem. Soc.*, 2016, **138**, 5821.

5 For selected book and reviews on synthesis of allenes, see: (*a*) N. Krause and A. S. K. Hashimi, in *Modern Allene Chemistry*, Wiley-VCH, Weinheim, 2004, vol. 1; (*b*) N. Krause and A. Hoffmann-Röder, *Tetrahedron*, 2004, **60**, 11671; (*c*) G. B. Hammond, in *Fluorine-Containing Synthons*, 2005, pp. 204–215; (*d*) K. Brummond and J. DeForrest, *Synthesis*, 2007, **2007**, 795; (*e*) M. Ogasawara, *Tetrahedron: Asymmetry*, 2009, **20**, 259; (*f*) S. Yu and S. Ma, *Chem. Commun.*, 2011, **47**, 5384; (*g*) R. K. Neff and D. E. Frantz, *ACS Catal.*, 2014, **4**, 519; (*h*) J. Ye and S. Ma, *Org. Chem. Front.*, 2014, **1**, 1210; (*i*) S. Shirakawa, S. Liu and S. Kaneko, *Chem.–Asian J.*, 2016, **11**, 330; (*j*) W.-D. Chu, Y. Zhang and J. Wang, *Catal. Sci. Technol.*, 2017, **7**, 4570; (*k*) M. L. Hossain and J. Wang, *Chem. Rec.*, 2018, **18**, 1548; (*l*) X. Huang and S. Ma, *Acc. Chem. Res.*, 2019, **52**, 1301.

6 For selected book and reviews on transformation of allenes, see: (*a*) N. Krause and A. S. K. Hashimi, in *Modern Allene Chemistry*, Wiley-VCH, Weinheim, 2004, vol. 2; (*b*) X. Zhang and S. Ma, in *Fluorination, Synthetic Organofluorine Chemistry*, Springer, Singapore, 2019, vol. 1, pp. 1–16; (*c*) R. Zimmer, C. U. Dinesh, E. Nandanan and F. A. Khan, *Chem. Rev.*, 2000, **100**, 3067; (*d*) S. Ma, *Acc. Chem. Res.*, 2003, **36**, 701; (*e*) L. K. Sydnes, *Chem. Rev.*, 2003, **103**, 1133; (*f*) S. Ma, *Chem. Rev.*, 2005, **105**, 2829; (*g*) Ref. 5c; (*h*) M. Brasholz, H. U. Reissig and R. Zimmer, *Acc. Chem. Res.*, 2009, **42**, 45; (*i*) S. Ma, *Acc. Chem. Res.*, 2009, **42**, 1679; (*j*) S. Yu and S. Ma, *Angew. Chem., Int. Ed.*, 2012, **51**, 3074; (*k*) T. Lu, Z. Lu, Z. X. Ma, Y. Zhang and R. P. Hsung, *Chem. Rev.*, 2013, **113**, 4862; (*l*) J. Ye and S. Ma, *Acc. Chem. Res.*, 2014, **47**, 989; (*m*) F. López and J. L. Mascareñas, *Chem. Soc. Rev.*, 2014, **43**, 2904; (*n*) B. Alcaide, P. Almendros and C. Aragoncillo, *Chem. Soc. Rev.*, 2014, **43**, 3106; (*o*) M. P. Muñoz, *Chem. Soc. Rev.*, 2014, **43**, 3164; (*p*) M. Holmes, L. A. Schwartz and M. J. Krische, *Chem. Rev.*, 2018, **118**, 6026; (*q*) Y. Liu and M. Bandini, *Chin. J. Chem.*, 2019, **37**, 431; (*r*) L. Liu, R. M. Ward and J. M. Schomaker, *Chem. Rev.*, 2019, **119**, 12422.

7 T. Fujihara, T. Hosomi, C. Cong, T. Hosoki, J. Terao and Y. Tsuji, *Tetrahedron*, 2015, **71**, 4570.

8 For selected reviews on hydrometalation of allenes, see: (*a*) A. P. Pulis, K. Yeung and D. J. Procter, *Chem. Sci.*, 2017, **8**, 5240; (*b*) J. Chen, J. Guo and Z. Lu, *Chin. J. Chem.*, 2018, **36**, 1075; (*c*) T. Fujihara and Y. Tsuji, *Synthesis*, 2018, **50**, 1737.

9 A. Sawada, T. Fujihara and Y. Tsuji, *Adv. Synth. Catal.*, 2018, **360**, 2621.

10 For non-enantioselective hydrocupration of allenes, see: (*a*) Y. Tani, K. Kuga, T. Fujihara, J. Terao and Y. Tsuji, *Chem. Commun.*, 2015, **51**, 13020; (*b*) R. Y. Liu, Y. Yang and S. L. Buchwald, *Angew. Chem., Int. Ed.*, 2016, **55**, 14077; (*c*) T. Fujihara, K. Yokota, J. Terao and Y. Tsuji, *Chem. Commun.*, 2017, **53**, 7898; (*d*) M. Lee, M. Nguyen, C. Brandt, W. Kaminsky and G. Lalic, *Angew. Chem., Int. Ed.*, 2017, **56**, 15703; (*e*) R. K. Klake, S. L. Gargaro, S. L. Gentry, S. O. Elele and J. D. Sieber, *Org. Lett.*, 2019, **21**, 7992.

11 For non-enantioselective borylcupration of allenes, see: (*a*) J. Rae, K. Yeung, J. J. W. McDouall and D. J. Procter, *Angew. Chem., Int. Ed.*, 2016, **55**, 1102; (*b*) W. Yuan, L. Song and S. Ma, *Angew. Chem., Int. Ed.*, 2016, **55**, 3140; (*c*) W. Zhao and J. Montgomery, *J. Am. Chem. Soc.*, 2016, **138**, 9763; (*d*) Y.-S. Zhao, X.-Q. Tang, J.-C. Tao, P. Tian and G.-Q. Lin, *Org. Biomol. Chem.*, 2016, **14**, 4400; (*e*) A. Boreux, K. Indukuri, F. Gagosz and O. Riant, *ACS Catal.*, 2017, **7**, 8200; (*f*) T. Fujihara, A. Sawada, T. Yamaguchi, Y. Tani, J. Terao and Y. Tsuji, *Angew. Chem., Int. Ed.*, 2017, **56**, 1539; (*g*) L. Song, W. Yuan and S. Ma, *Org. Chem. Front.*, 2017, **4**, 1261; (*h*) Y. Ozawa, H. Iwamoto and H. Ito, *Chem. Commun.*, 2018, **54**, 4991; (*i*) J. Chen, S. Gao and M. Chen, *Chem. Sci.*, 2019, **10**, 10601; (*j*) J. Chen, S. Gao and M. Chen, *Org. Lett.*, 2019, **21**, 8800; (*k*) K. Yeung, F. J. T. Talbot, G. P. Howell, A. P. Pulis and D. J. Procter, *ACS Catal.*, 2019, **9**, 1655.

12 For enantioslelective hydrocupration of allenes, trapping with ketones, see: (*a*) E. Y. Tsai, R. Y. Liu, Y. Yang and S. L. Buchwald, *J. Am. Chem. Soc.*, 2018, **140**, 2007; (*b*) R. Y. Liu, Y. Zhou, Y. Yang and S. L. Buchwald, *J. Am. Chem. Soc.*, 2019, **141**, 2251; (*c*) S. L. Gargaro, R. K. Klake, K. L. Burns, S. O. Elele, S. L. Gentry and J. D. Sieber, *Org. Lett.*, 2019, **21**, 9753, trapping with carbon dioxide, see: (*d*) J. Qiu, S. Gao, C. Li, L. Zhang, Z. Wang, X. Wang and

 This journal is © The Royal Society of Chemistry 2020

Open Access Article. Published on 22 July 2020. Downloaded on 2/7/2026 4:41:18 PM.
This article is licensed under a Creative Commons Attribution-NonCommercial 3.0 Unported Licence.

K. Ding, *Chem.–Eur. J.*, 2019, **25**, 13874, trapping with allylic phosphates, see: (*e*) Y. Sun, Y. Zhou, Y. Shi, J. del Pozo, S. Torker and A. H. Hoveyda, *J. Am. Chem. Soc.*, 2019, **141**, 12087; (*f*) G. Xu, B. Fu, H. Zhao, Y. Li, G. Zhang, Y. Wang, T. Xiong and Q. Zhang, *Chem. Sci.*, 2019, **10**, 1802, trapping with intramolecular enones, see: (*g*) Y.-X. Tan, X.-Q. Tang, P. Liu, D.-S. Kong, Y.-L. Chen, P. Tian and G.-Q. Lin, *Org. Lett.*, 2018, **20**, 248, trapping with indazoles, see: (*h*) Y. Ye, I. Kevlishvili, S. Feng, P. Liu and S. L. Buchwald, *J. Am. Chem. Soc.*, 2020, **142**, 10550.

13 For enantioslelective borylcupration of allenes, trapping with imines, see: (*a*) H. Jang, F. Romiti, S. Torker and A. H. Hoveyda, *Nat. Chem.*, 2017, **9**, 1269; (*b*) H. Deng, Z. Meng, S. Wang, Z. Zhang, Y. Zhang, Y. Shangguan, F. Yang, D. Yuan, H. Guo and C. Zhang, *Adv. Synth. Catal.*, 2019, **361**, 3582, trapping with acyl fluorides, see: (*c*) J. Han, W. Zhou, P.-C. Zhang, H. Wang, R. Zhang, H.-H. Wu and J. Zhang, *ACS Catal.*, 2019, **9**, 6890, trapping with nitriles, see: (*d*) S. Zhang, J. del Pozo, F. Romiti, Y. Mu, S. Torker and A. H. Hoveyda, *Science*, 2019, **364**, 45, trapping with α,β,γ,δ-unsaturated diesters, see: (*e*) Y. Huang, S. Torker, X. Li, J. delPozo and A. H. Hoveyda, *Angew. Chem., Int. Ed.*, 2019, **58**, 2685.

14 For selected reviews on construction of quarternary carbon centers, see: (*a*) Y. Li and S. Xu, *Chem.–Eur. J.*, 2018, **24**, 16218; (*b*) H. Li and Y. Lu, *Asian J. Org. Chem.*, 2017, **6**, 1130; (*c*) X. P. Zeng, Z. Y. Cao, Y. H. Wang, F. Zhou and J. Zhou, *Chem. Rev.*, 2016, **116**, 7330; (*d*) L. Tian, Y.-C. Luo, X.-Q. Hu and P.-F. Xu, *Asian J. Org. Chem.*, 2016, **5**, 580; (*e*) K. W. Quasdorf and L. E. Overman, *Nature*, 2014, **516**, 181.

15 For selected reviews on construction of quarternary carbon centers in acyclic systems, see: (*a*) J. Feng, M. Holmes and M. J. Krische, *Chem. Rev.*, 2017, **117**, 12564; (*b*) J. P. Das and I. Marek, *Chem. Commun.*, 2011, **47**, 4593.

16 For selected examples on asymmetric synthesis of α-all-carbon-quarternary β,γ-unsaturated carbonyl compounds, see: (*a*) P. A. Evans, S. Oliver and J. Chae, *J. Am. Chem. Soc.*, 2012, **134**, 19314; (*b*) P. A. Evans and S. Oliver, *Org. Lett.*, 2013, **15**, 5626; (*c*) B. W. H. Turnbull, S. Oliver and P. A. Evans, *J. Am. Chem. Soc.*, 2015, **137**, 15374; (*d*) K. Hojoh, H. Ohmiya and M. Sawamura, *J. Am. Chem. Soc.*, 2017, **139**, 2184; (*e*) S. E. Shockley, J. C. Hethcox and B. M. Stoltz, *Angew. Chem., Int. Ed.*, 2017, **56**, 11545.

17 J. Li, C. Zhou, C. Fu and S. Ma, *Tetrahedron*, 2009, **65**, 3695.

18 F. Chen, F.-F. Zhu, M. Zhang, R.-H. Liu, W. Yu and B. Han, *Org. Lett.*, 2017, **19**, 3255.

19 (*a*) M.-K. Zhu, J.-F. Zhao and T.-P. Loh, *J. Am. Chem. Soc.*, 2010, **132**, 6284; (*b*) B. Han, X.-L. Yang, R. Fang, W. Yu, C. Wang, X.-Y. Duan and S. Liu, *Angew. Chem., Int. Ed.*, 2012, **51**, 8816; (*c*) X.-L. Yang, F. Chen, N.-N. Zhou, W. Yu and B. Han, *Org. Lett.*, 2014, **16**, 6476.

20 K. E. Kim, J. Li, R. H. Grubbs and B. M. Stoltz, *J. Am. Chem. Soc.*, 2016, **138**, 13179.